JACS
JOURNAL OF THE AMERICAN CHEMICAL SOCIETY
pubs.acs.org/JACS
Article

Amide-Based Naphthotubes as Biomimetic Receptors for Acetal Protection and Other Substrates in Water via Noncovalent Interactions

Hang Zhou, Xin-Yu Pang, Xiaojiang Xie, David Lee Phillips,* Han-Yuan Gong,* Jonathan L. Sessler,* and Wei Jiang

Cite This: J. Am. Chem. Soc. 2024, 146, 34842−34851

Read Online

ACCESS | Metrics & More | Article Recommendations | Supporting Information

ABSTRACT: Active compound protection can allow inherently unstable molecules to be stabilized and latent reactivity to be masked. Synthetic receptors are attractive in terms of providing such protection. Nevertheless, preserving the activity and functionality of organic molecules in water poses a challenge. Here, we show that biomimetic receptors, specifically amide naphthotubes and an amide anthryltube, allow the efficient preservation of functional organic molecules in water. In particular, the amide naphthotubes were found to extend the half-lives of acetal-containing substrates ("acetals") against acid-catalyzed hydrolysis by up to 3000 times. This kinetic protection effect was ascribed to hydrogen bond-based recognition of the organic guests. A substrate dependence was seen that was further exploited to achieve the kinetic resolution of acetal isomers. To the best of our knowledge, the present study constitutes one of the most effective acetal protection strategies reported to date. The recognition-based protection approach reported here appears generalizable as evidenced by the protection of eight different substrates against six distinct chemical reactions. Based on the present findings, we propose that it is possible to design receptors that provide for the protection of specific substrates under a variety of reaction conditions including those carried out in water.

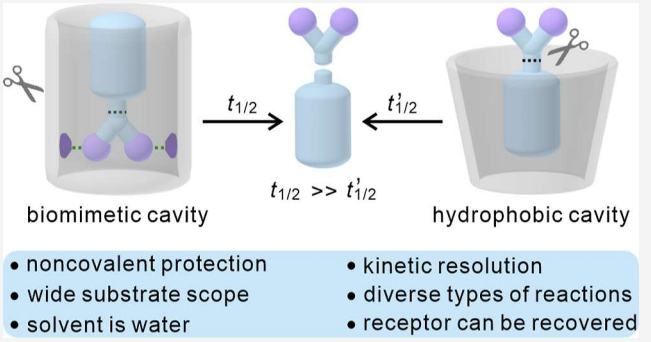

INTRODUCTION

The preservation of active species against undesirable chemical transformations is important in areas as diverse as synthetic chemistry,[1,2] chemical biology,[3,4] pharmaceutical science,[5,6] and material science.[7,8] Conventional protection methods require the covalent modification of active groups in order to temporarily mask their inherent reactivity. Unfortunately, this time-honored approach is often plagued by high costs, inefficiencies associated with selecting the optimal protecting group, as well as the labor associated with carrying out the necessary protection and deprotection steps.[9] Noncovalent protection, which relies on host−guest complexation, constitutes an attractive complementary strategy.[10−12] Here, protection involves substrate capture by a receptor followed by controlled rerelease. In favorable cases, the recognition and release events are readily triggered by external stimuli and the requisite receptors are both stable and readily accessible.

Previous studies with synthetic receptors have served to highlight their ability to effect noncovalent molecular protection,[13−19] regulate reactivity,[20−23] enable site−selective reactions,[24−26] and facilitate the kinetic resolution of isomers.[27−31] However, achieving the noncovalent protection of active molecules in water using synthetic receptors remains a largely unmet challenge.[13,17,22,23,28] This stands in contrast to bioreceptors that shield active molecules (i.e., guests) from the surrounding solution via their strategic inclusion within specific binding pockets (Figure 1a).[32] The protection of substrates can be further enhanced by anchoring their constituent polar groups within the pockets of bioreceptors through noncovalent interactions.[33]

At present, the majority of synthetic receptors that are soluble in water do not possess polar binding sites within their hydrophobic cavity.[34−38] As a consequence, they display a binding preference wherein the nonpolar portions of a guest molecule are bound within the receptor, while polar group(s) remain exposed to the surrounding aqueous medium (Figure 1b). Full enclosure of the entire guest molecule (Figure 1c), rather than selectively binding only the polar groups within the

Received: October 4, 2024
Revised: November 15, 2024
Accepted: November 19, 2024
Published: December 5, 2024

https://doi.org/10.1021/jacs.4c13907
J. Am. Chem. Soc. 2024, 146, 34842−34851

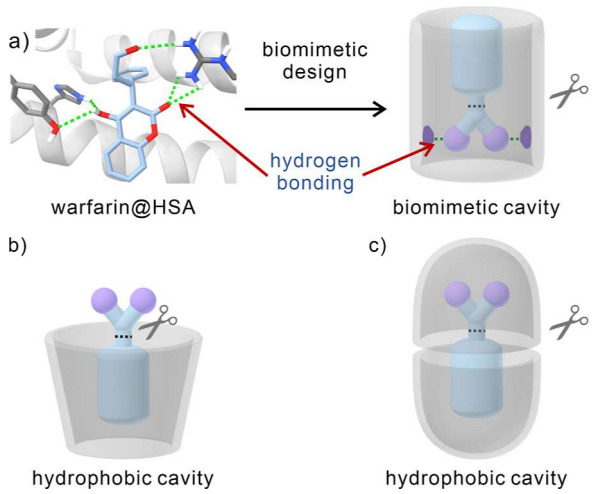

Figure 1. Schematic representation of noncovalent protection of functional organic molecules in water: (a) Recognition and protection by a bioreceptor or a biomimetic cavity. (b, c) Recognition and protection by hydrophobic cavities.

cavity, is also frequently seen. A limited number of synthetic receptors possessing hydrophobic pockets with polar binding sites are known.[39−49] However, to our knowledge, there is only a single report where a synthetic receptor system possessing polar binding sites has been employed for noncovalent protection in aqueous environments.[26] Moreover, the scope of applicable substrates was limited to acid-sensitive isonitriles.

Here, we show that biomimetic receptors, specifically amide naphthotubes designated as **1** and **2** (shown in Figure 2a), as well as an amide anthryltube **4** (shown in Figure 8), allow the efficient protection of functional organic molecules in water against canonical reactions to which they are prone. As detailed below, the naphthotubes **1a** and **1b** proved effective in recognizing acetal-containing substrates ("acetals") in water, as well as inhibiting their acid-catalyzed hydrolysis (up to 3000-fold). Using both the amide naphthotubes **2a** and **2b** and the amide anthryltube **4**, the potential generality of this noncovalent protection strategy was demonstrated with eight distinct substrates across six different chemical reactions. Structural evidence for substrate binding was obtained using analogue **3** (shown in Figure 2a).

RESULTS AND DISCUSSION

Interactions between Amide Naphthotubes and Acetals in Water. Acetal compounds are widely utilized protecting groups for carbonyl moieties and can serve as responsive components in smart materials.[1,2,50] Acetal moieties also appear in several drugs.[51] Acetals as a class are known for their stability in basic and neutral environments; however, hydrolysis is facile in aqueous acid (Figure 2b). Enhancing the stability of acetals in acidic solutions is expected to expand the range of their applications. Although several synthetic receptors are able to bind acetals and accelerate effectively their hydrolysis,[52−55] stabilizing acetals to hydrolysis through use of an artificial receptor remains an unmet challenge. We felt that this challenge could be met through use of amide naphthotubes.

In previous work, we showed that amide naphthotubes of general structure **2** (Figure 2a) act as biomimetic receptors that selectively bind polar organic molecules in water.[56−61] This ability was ascribed to the fact that they possess

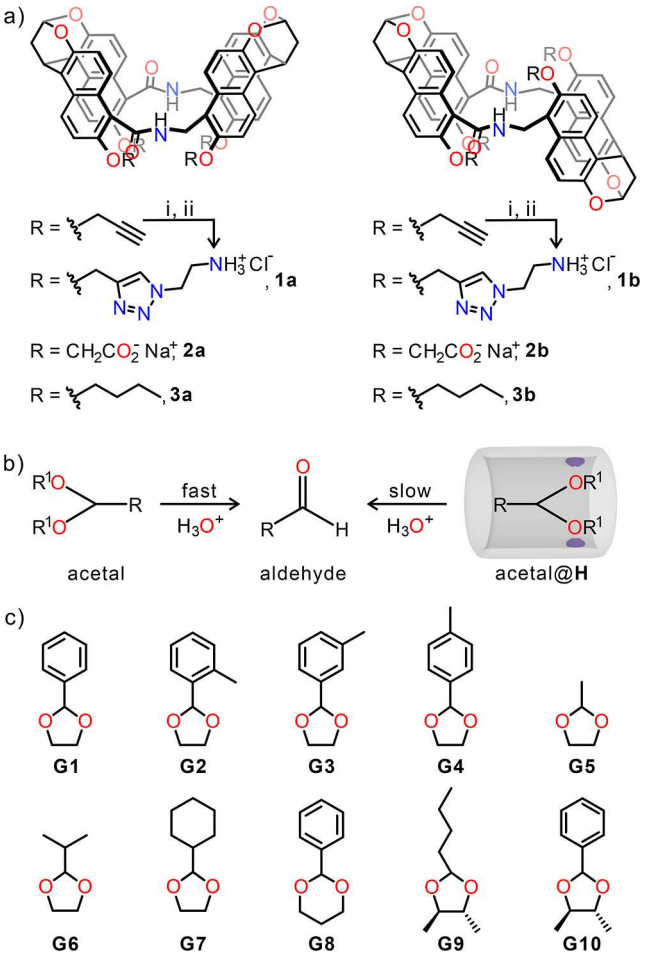

Figure 2. (a) Synthesis of amide naphthotubes **1a** and **1b** (designated as **H**). (i) $[Cu(CH_3CN)_4]^+PF_6^-$, $N_3(CH_2)_2NHBoc$, CH_2Cl_2, r.t., 12 h; (ii) HCl, THF/H_2O, r.t., 12 h. (b) Acid-catalyzed hydrolysis of acetals. (c) Chemical structures of acetals considered in this study (designated as **G1−G10**).

hydrophobic cavities endowed with two inwardly oriented hydrogen-bonding donors. The two classes of amide naphthotubes considered in this study, represented by **1a−3a** and **1b−3b**, have shapes and binding sites that were expected to be complementary to acetal-containing substrates. This led us to test their ability to provide for supramolecular-based protection for acetal compounds under conditions that would otherwise favor hydrolysis.

In order to provide protection in water, we deemed it necessary to create amide naphthotubes that were soluble in acidic aqueous media. Derivatives **1a** and **1b** (Figure 2a), were thus synthesized. Here, so-called click chemistry was used to convert a pair of amide naphthotubes containing alkyne side chains into ones containing solubilizing primary ammonium groups.[60] Both **1a** and **1b** were obtained in yields exceeding 80% and fully characterized via NMR spectroscopy and mass spectrometry (see Supporting Information, Figures S1−S10).

Prior to testing the present amide naphthotubes as noncovalent acetal protecting groups, efforts were made to test their host−guest binding characteristics. A range of acetal compounds with different substituents (**G1−G10**, Figure 2c) were synthesized (Figures S11−S26) and used for these tests. Unfortunately, no pH conditions could be found where receptors **1a** and **1b** were both monodisperse and soluble (i.e.,

https://doi.org/10.1021/jacs.4c13907
J. Am. Chem. Soc. 2024, 146, 34842−34851

pH ≤ 4.6) and where acetal hydrolysis was sufficiently slow as to allow establishment of a bona fide equilibrium. Given this, analogues **2a** and **2b** were used to investigate the binding properties of the naphthotubes in a basic aqueous medium.[57] The binding cavities of **2a** and **2b** are identical to those of **1a** and **1b** with the only difference being the side chains. These side chains being reasonably well separated from the binding cavity were not expected to have a substantial impact on the binding characteristics. Support for this supposition comes from the finding that similar binding constants are observed for 1,4-dioxane, a representative neutral guest. Specifically, a binding constant of 2.0×10^3 M^{-1} was found for **1a** (Figures S27 and S28). This value matches well the 3.2×10^3 M^{-1} seen for **2a**.[58] Likewise, **1b** displays a binding constant of 1.2×10^4 M^{-1} for 1,4-dioxane that is comparable to the 1.4×10^4 M^{-1} seen for **2b** (Figures S29 and S30).[58]

The ^{1}H NMR spectra of solutions containing 1:1 mixtures of naphthotubes **2a** and **2b** and various acetal-containing substrates revealed notable proton signal shifts compared to the free hosts and guests. This is taken as evidence of the binding interactions between the naphthotubes and the acetals (Figures S31−S50). The association constants were determined by means of fluorescence spectroscopic titration (Figures S51−S70) and are summarized in Table 1.

Table 1. Association Constants ($K_a/10^4$, M^{-1}) of Amide Naphthotubes 2a and 2b with G1−G10 in H_2O at 298 K and pH = 7.0, as Determined by Fluorescence Spectroscopic Titrations[a]

	G1	G2	G3	G4	G5
2a	51 ± 2	9.6 ± 0.1	41 ± 3	76 ± 1	0.9 ± 0.1
2b	210 ± 10	6.0 ± 0.1	290 ± 20	540 ± 20	1.6 ± 0.1
	G6	**G7**	**G8**	**G9**	**G10**
2a	3.3 ± 0.2	22 ± 2	2.5 ± 0.1	19 ± 2	0.3 ± 0.1
2b	7.8 ± 0.4	150 ± 20	23 ± 1	12 ± 2	5.6 ± 0.3

[a]Value is the average of three independent measurements.

Based on the determined binding constants, amide naphthotubes **2a** and **2b** bind most acetal guests effectively in water at pH = 7.0. Acetal compounds with larger hydrophobic substituents, such as aromatic groups (**G1**, **G4**, **G8**) and a cyclohexyl group (**G7**), display enhanced affinities toward these water-soluble naphthotubes. The association constant observed for **G4** (5.4×10^6 M^{-1}) is relatively high for a synthetic host operating in water and is noteworthy given the relatively small size of **G4**.[62] As a general rule, naphthotube **2b** exhibits a higher affinity for any given guest than **2a**. While not a proof, this difference is readily rationalized in terms of the presence of a deeper hydrophobic cavity in the case of **2b**.[59]

The binding interaction between the amide naphthotubes and acetals guests was explored in the solid state via single crystal X-ray diffraction analysis. The high solubility of **1** and **2** in water stymied efforts to grow diffraction single crystals of acetal-containing host−guest complexes. Fortunately, several single crystals of host−guest complexes suitable for X-ray crystallographic study were obtained from CH_2Cl_2 using analogues **3a** and **3b** as the hosts[58] (Figure 3). In the structure of **G1@3b**, the acetal moiety of **G1** is included in the cavity of **3b** and stabilized via two apparent N−H···O hydrogen bonds characterized by N−O distances of ca. 2.9 Å. Both **G4** and **G7** contain an acetal group similar to **G1**, but with different substituents. **G4** has a bulkier *p*-tolyl group, while **G7** has a cyclohexyl moiety. Analyses of crystals of **G4@3b** and **G7@3b** revealed a binding geometry comparable to that seen in **G1@3b**. Furthermore, despite the presence of a larger acetal moiety (1,3-dioxane) in **G8**, the crystal structure of **G8@3b** is again characterized by the existence of two N−H···O hydrogen bonds as inferred from an N−O separation of less than 3.0 Å. Density functional theory (DFT) calculations were also carried out on **G1@1a** and **G1@1b** in water (Figures S71 and S72). The results are interpreted in terms of hydrogen bond interactions playing a key role in stabilizing the complexes formed between the naphthotubes **1a** and **1b** and acetal **G1**. More broadly, both the crystal structures and the calculations provide support for the conclusion that acetal-containing substrates can be bound within the cavities of the amide-containing naphthotubes **1**−**3**.

Protection of Acetal Compounds. Using amide naphthotubes **1a** and **1b** as the receptors, we tested whether the biomimetic recognition inferred on the basis of the above studies could be used to protect acetals in acidic aqueous environments. Benzaldehyde glycol acetal **G1** was selected as the acetal substrate for the initial study, primarily due to the extensive use of the 1,3-dioxolane moiety as a protecting group in synthesis and the common occurrence of the phenyl group in a variety of organic compounds. Two additional water-soluble macrocyclic receptors, namely *β*-cyclodextrin (*β*-CD) and cucurbit[7]uril (CB[7]), were chosen as host molecules to allow receptor-based comparisons. These two control systems have hydrophobic cavities that lack inner polar moieties that could serve as potential acetal binding sites; indeed, they generally bind guests through inferred hydrophobic interactions.[63−66] In aqueous solution, *β*-CD and CB[7] bind **G1** with association constants (K_a) of 310 and 260 M^{-1}, respectively (Figures S73−S76). The binding modes revealed by DFT calculation (Figures S77 and S78) and reference to the literature[63−66] served to confirm that both *β*-CD and CB[7] display a binding preference for the hydrophobic phenyl group of **G1**, thus leaving the hydrophilic 1,3-dioxolane moiety exposed to the surrounding aqueous medium.

The hydrolysis of **G1** (0.25 mM) was monitored via ^{1}H NMR spectroscopy in the absence and presence of **1a**, **1b**, *β*-CD, and CB[7] (1.0 molar equiv in all cases). Here, a pD = 4.4 was maintained by means of an acetate buffer (50 mM) at 298 K (cf. Figure 4, and Figures S79−S92). The reaction progress was evaluated by monitoring the change in the integrated value of the proton signals corresponding to the glycol product. In the absence of a synthetic receptor, **G1** was completely hydrolyzed to the limits of detection within 12 h (Figure 4). The calculated half-life ($t_{1/2\text{-free}}$ = 2.6 h) and rate constant (k_{obs} = 7.5×10^{-5} s^{-1}) were obtained by fitting the kinetic data to a model predicated on pseudo-first-order kinetics.

In accord with our design expectations, the presence of either **1a** or **1b** in this buffered acidic aqueous solution of **G1** led to a noticeable reduction in the hydrolysis rate. Specifically, over a period of 12 h, less than 15% and 5% of **G1** underwent hydrolysis in the presence of 1.0 molar equiv of **1a** and **1b**, respectively. The half-lives of **G1** exposed to 1.0 molar equiv of **1a** or **1b** were $t_{1/2\text{-bound}}$ = 31.2 h, and $t_{1/2\text{-bound}}$ > 160 h, respectively. These findings are taken as evidence of a notable enhancement in the stability of **G1**. In contrast, neither *β*-CD nor CB[7] proved effective in preventing the hydrolysis of **G1**. In fact, the presence of CB[7] was found to accelerate the hydrolysis of **G1**. The result is consistent with prior reports

https://doi.org/10.1021/jacs.4c13907
J. Am. Chem. Soc. 2024, 146, 34842−34851

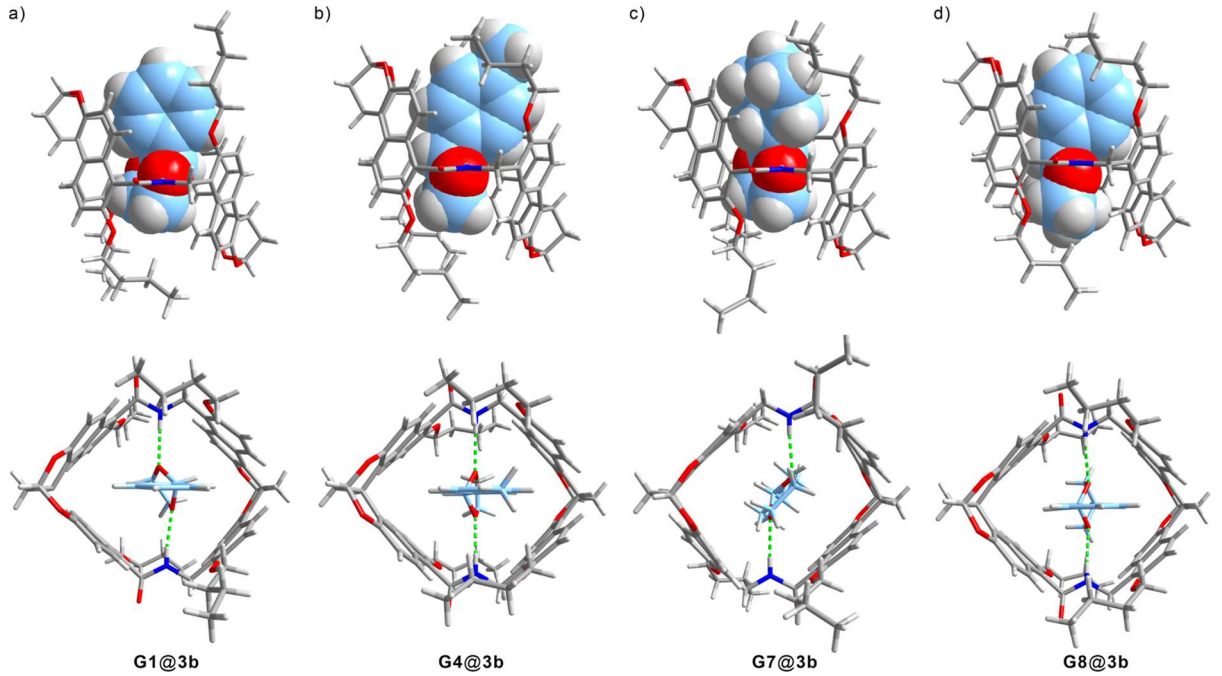

Figure 3. Side and top views of the single crystal X-ray diffraction structures of (a) **G1@3b**, (b) **G4@3b**, (c) **G7@3b**, and (d) **G8@3b**. Green dotted lines indicate presumed intermolecular N−H···O hydrogen bonds.

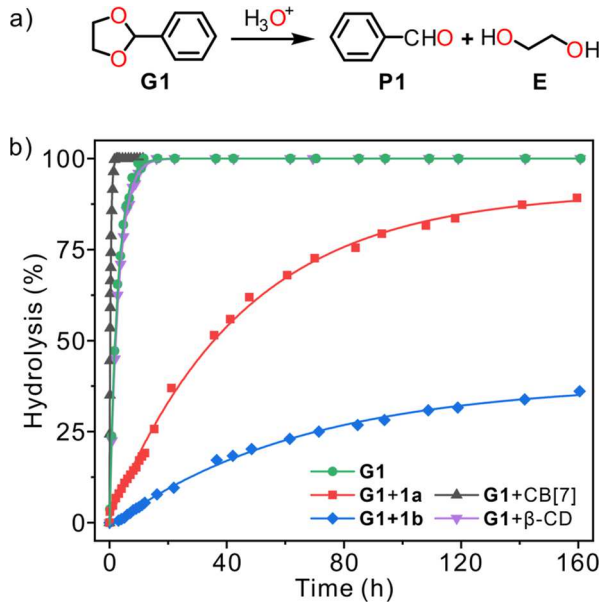

Figure 4. (a) Acid-catalyzed hydrolysis of acetal **G1**. (b) Kinetic traces corresponding to the hydrolysis of **G1** (0.25 mM) at pD = 4.4 and 298 K in the absence and presence of 1.0 molar equiv of various synthetic receptors, namely **1a**, **1b**, *β*-CD, and CB[7]. Solid lines represent fitting to model kinetic curves highlighting the influence of each receptor on the hydrolysis rates.

that CB[7] can promote the acid-catalyzed hydrolysis of various substrates.[53,67] The contrast between the protection provided by **1a** and **1b** relative to *β*-CD or CB[7] underscores the role naphthotubes can play in both acetal binding and protection in aqueous media.

To investigate further the protective effects of naphthotubes **1a** and **1b** on **G1**, a series of hydrolysis tests were carried out using conditions expected to accelerate acetal hydrolysis (Table 2, and Figures S93−S108). The results indicate that

Table 2. Half-lives of G1 at pD = 4.4 and pD = 2.8 in the Absence ($t_{1/2\text{-free}}$, h) and Presence ($t_{1/2\text{-bound}}$, h) of Synthetic Receptors (1a, 1b, *β*-CD, or CB[7]), and the Corresponding Protection Ratios α ($\alpha = t_{1/2\text{-bound}}/t_{1/2\text{-free}}$)

H	pD	[H]/[G1]	$t_{1/2\text{-free}}$	$t_{1/2\text{-bound}}$	α
1a	4.4	1	2.6	31.2	12
1b	4.4	1	2.6	>160	>61
β-CD	4.4	1	2.6	2.9	1.1
CB[7]	4.4	1	2.6	0.3	0.1
1a	4.4	2	2.6	110	42
1a	2.8	1	0.05	18.1	362
1a	2.8	2	0.05	59.5	1190
1b	2.8	1	0.05	30.3	606
1b	2.8	2	0.05	150	3000

the protection relative to receptor-free controls becomes enhanced as the baseline hydrolysis rate increases. For instance, the protection ratio (α, where $\alpha = t_{1/2\text{-bound}}/t_{1/2\text{-free}}$) in the presence of 1.0 molar equiv of **1a** at pD = 2.8 is 30 times higher than that at pD = 4.4. Moreover, the protection level can be controlled via modifying the concentration of **1a** or **1b**. At a pD value of 4.4, an increase in the concentration of **1a** from 1.0 to 2.0 molar equiv resulted in an increase in the protection ratio from 12 to 42. Similar concentration-based trends were observed in the presence of **1a** or **1b** at pD = 2.8. In fact, using 2.0 molar equiv of **1a** or **1b** at pD = 2.8, protection ratios of α = 1190 and 3000 were noted for **1a** and **1b**, respectively. Although specific comparisons are subject to caveats related to conditions, such as substrate type, solvent, and temperature, to the best of our knowledge, these values represent the most efficient acetal protection reported to date.

An analysis of the hydrolysis kinetics was performed in an effort to obtain a deeper understanding of the protection mechanism. As illustrated in Figure 5, in the presence of a host molecule, **G1** was considered likely to undergo hydrolysis via two limiting mechanistic pathways. Model A postulates that

https://doi.org/10.1021/jacs.4c13907
J. Am. Chem. Soc. 2024, 146, 34842−34851

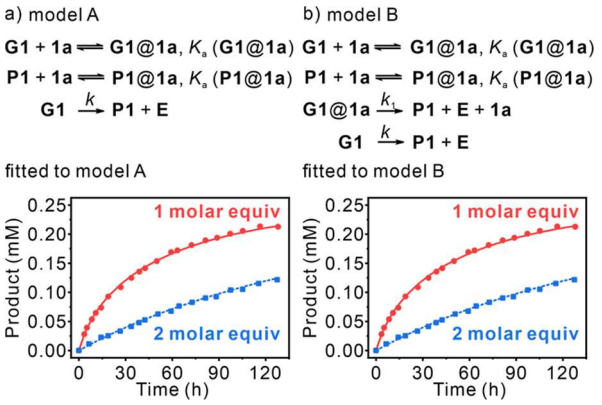

Figure 5. Kinetic models and plots of the concentration of the benzaldehyde product **P1** vs time for the acid-catalyzed hydrolysis of **G1** in the presence of **1a** at pD = 4.4 showing the equations, fitting, and simulation corresponding to model A (a), and model B (b). Red circles and blue squares represent the experimental data in the presence of 1.0 molar equiv and 2.0 molar equiv of **1a**, respectively. Red solid lines represent the fit of the hydrolysis data of **G1** in the presence of 1.0 molar equiv of **1a**. Blue dash lines represent the simulation of the hydrolysis of **G1** in the presence of 2.0 molar equiv of **1a**.

the hydrolysis of **G1** takes place solely within the bulk solution, whereas model B is predicated on the assumption that **G1** hydrolysis occurs both internal and external to the host cavity. To determine which model, if either, provides the best description, the kinetic data corresponding to the hydrolysis of **G1** in the presence of 1.0 molar equiv of the amide naphthotube **1a** at a pD value of 4.4 was used to determine the binding constant K_a(**G1@1a**) and the reaction rate k_1. Both parameters were then used to model the hydrolysis of **G1** with 2.0 molar equiv of **1a**. Finally, a comparison was made between the experimental and simulated kinetic data. To simplify the fitting process and reduce the number of parameters, the experimentally determined values of the association constant K_a(**P1@1a**) = 5.6×10^3 M^{-1} and the rate constant $k = 7.5 \times 10^{-5}$ s^{-1} were fixed during the calculation of the binding constant between the benzaldehyde product **P1** and **1a**, as well as the hydrolysis rate of bound **G1** at pD 4.4. This approach enhances the accuracy and reliability of the model by minimizing the number of fitting parameters.

Per the above, the hydrolysis data of **G1** with 1.0 molar equiv of **1a** were fitted to model A. This gave K_a(**G1@1a**) = $(1.7 \pm 0.1) \times 10^5$ M^{-1} (Figure 5). The hydrolysis of **G1** in the presence of 2.0 molar equiv of **1a** was then simulated using model A. The resulting parameters were found to match well to the experimental results, as indicated by a R^2 value of 0.9989 and a root-mean-square error (RMSE) value of 2.20×10^{-6} in comparing the simulated and experimental kinetic data points. Likewise, the hydrolysis data for **G1** in the presence of 1.0 molar equiv of **1a** was fitted to model B giving a K_a(**G1@1a**) value of $(1.8 \pm 0.1) \times 10^5$ M^{-1} and $k_1 = (7.5 \pm 2.7) \times 10^{-8}$ s^{-1}. Based on model B, the calculated hydrolysis data for **G1** in the presence of 2.0 molar equiv of **1a** closely matched the experimental data, as evidenced by $R^2 = 0.9990$ and RMSE = 1.66×10^{-6} for a comparison between the simulated and experimental kinetic data points.

It is noteworthy that both models A and B provide acceptable fits to the experimental data. While model A assumes that the bound **G1** does not hydrolyze ($k_1 = 0$), model B includes terms for the hydrolysis of **G1** both inside and outside of the cavity ($k_1 \neq 0$). In fact, the hydrolysis rate of bound **G1** in model B ($k_1 = (7.5 \pm 2.7) \times 10^{-8}$ s^{-1} as noted above) is approximately one-thousandth of that of free **G1** hydrolysis ($k = 7.5 \times 10^{-5}$ s^{-1}) and is therefore considered negligible. Moreover, the binding constants derived from model A (K_a(**G1@1a**) = $(1.7 \pm 0.1) \times 10^5$ M^{-1}) and model B (K_a(**G1@1a**) = $(1.8 \pm 0.1) \times 10^5$ M^{-1}) are identical to one another within error and close to the K_a(**G1@2a**) value of 5.1×10^5 M^{-1} determined directly by experiment. In other words, because the rate of **G1** hydrolysis is greatly reduced within the cavity, models A and B converge to become equivalent. As a further check, a different hydrolysis model was derived that presumes the hydrolysis of **G1** occurs exclusively within the host cavity (Figure S109). This latter model proved inconsistent with the experimental data.

The hydrolysis data of **G1** with **1a** or **1b** at pD = 2.8 were examined using the same two models as above. Again, comparable outcomes were noted (Figures S110 and S111). All of these findings provide support for the design expectation underlying the present study, namely that acetal hydrolysis is inhibited within the biomimetic cavities of amide naphthotubes **1a** and **1b**.

A solvent isotope effect was observed in the present naphthotube-based protection system, with the hydrolysis of **G1** (0.5 mM) in the presence of 1 molar equiv of **1a** displaying an extended half-life in D_2O (pD 4.2) compared to H_2O/D_2O (9:1, *v*/*v*; pH 3.8) (Figures S112−S116). Specifically, the half-life of **G1** was 1.3 times longer in D_2O. This effect is likely due to stronger noncovalent interactions, such as hydrogen bonding[68−70] and the hydrophobic effect,[71,72] between **1a** and **G1** in D_2O. In alignment with this hypothesis, the binding affinity of compound **2a**—and by extension, compound **1a** (as discussed above)—for **G1** in D_2O is approximately 1.7 times higher than in H_2O (see Figure S117). These findings are taken as further evidence of the critical role both hydrogen bonding and the hydrophobic effect play in acetal protection in this system.

The generality of the naphthotube-based protection strategy was then evaluated using **G2**−**G10** as substrates (Figures S118−S182). As can be seen from the data collected in Table 3, in all cases the half-lives for hydrolysis were increased. A correlation between the binding affinity and the degree of protection (α) was observed. A higher binding affinity typically results in enhanced protection for substrates with comparable hydrolysis rates. Acetals **G2**−**G4** have similar structures and hydrolysis rates. The binding affinity of **2a**, and by inference **1a** (see discussion above) to **G4** is ca. 2-fold higher than that of **G3**, and 8-fold higher than that of **G2**. Consequently, at both pD 4.4 and 2.8, naphthotube **1a** exhibits the highest level of protection toward **G4**; it provides moderate protection to **G3**, and offers the least protection to **G2**. This trend correlates with the relative binding strengths seen for each of these guests in the case of analogue **2a**. On the other hand, substrate **G5**, which is miscible with water and thus poorly bound by the naphthotubes, benefited from only a 3−4 fold level of protection. Additionally, the naphthotubes were found to offer varying levels of protection to different acetal groups, with stronger protection observed for acetals with less steric hindrance. For instance, while **G8** and **G10** contain the same phenyl substituent as **G1**, they possess bulkier 1,3-dioxane and 4,5-dimethyl-1,3-dioxolane groups, respectively. Consequently, naphthotube **1a** provides greater protection for **G1** than for **G8**

https://doi.org/10.1021/jacs.4c13907
J. Am. Chem. Soc. 2024, 146, 34842−34851

Table 3. Half-lives of G2−G10 in the Absence ($t_{1/2\text{-free}}$, h) and Presence ($t_{1/2\text{-bound}}$, h) of 1.0 Molar Equiv of Amide Naphthotubes 1a or 1b and Corresponding Protection Ratios α ($\alpha = t_{1/2\text{-bound}}/t_{1/2\text{-free}}$)

G	H	pD	$t_{1/2\text{-free}}$	$t_{1/2\text{-bound}}$	α
G2	1a	4.4	0.6	3.2	5
G3	1a	4.4	1.3	15.6	12
G4	1a	4.4	0.4	8.8	22
G2	1a	2.8	1.2×10^{-2}	1.2	100
	1b	2.8	1.2×10^{-2}	0.2	17
G3	1a	2.8	2.3×10^{-2}	8.2	356
	1b	2.8	2.3×10^{-2}	22.5	978
G4	1a	2.8	9.3×10^{-3}	3.8	409
	1b	2.8	9.3×10^{-3}	7.5	806
G5	1a	2.8	9.6	28.4	3
	1b	2.8	9.6	38.7	4
G6	1a	2.8	6.4	49.0	8
	1b	2.8	6.4	49.0	8
G7	1a	2.8	2.9	>180.0	>62
	1b	2.8	2.9	>180.0	>62
G8	1a	2.8	0.2	1.6	8
	1b	2.8	0.2	4.7	24
G9	1a	2.8	8.3	>240.0	>29
	1b	2.8	8.3	>240.0	>29
G10	1a	4.4	0.4	0.7	2
	1b	4.4	0.4	1.1	3

at pD 2.8, and similarly, stronger protection for **G1** over **G10** at pD 4.4. Collectively, these findings provide support for the suggestion that a wide variety of acetals can be protected using the present naphthotube-based strategy. However, the level of protection is substrate dependent.

Kinetic Resolution of Acetal Compounds. The substrate-dependent nature of the protection effect led us to explore whether the kinetic resolution of acetal isomers could be achieved using amide naphthotubes **1a** and **1b**. In the absence of a receptor, the constitutionally isomeric acetals **G2**−**G4** were found to display similar hydrolysis rates, thus precluding their resolution through chemical "loss" of the acetal functionality (cf. Figure S183). The presence of naphthotubes **1a** and **1b** was expected to perturb this baseline. To test this hypothesis, kinetic resolution experiments were carried out using various combinations of **G2**−**G4** and **1a** and **1b** (Figures S184−S189). The kinetic resolution of **G2** and **G4** with **1b** provides a representative example. In this study, a 1:1 mixture of **G2** and **G4** (0.25 mM in each) was added to an acidic solution (pD = 2.8) containing 0.25 mM **1b** (Figure 6a, Figures S186 and S187). The resulting solution was extracted rapidly with CD_2Cl_2 after stirring at 298 K for 5 min. After treating with Na_2CO_3 and Na_2SO_4 to effect neutralization and drying, respectively, the ^{1}H NMR spectrum of the organic phase was recorded and the percentage residual acetal determined.

The kinetic resolution studies revealed that both **1a** and **1b** can be employed for the kinetic resolution of acetal isomers (Figure 6b and Table S1). The effect is highly correlated with the binding affinity. It is not possible to obtain an effective kinetic resolution if two acetal isomers show similar association constants (e.g., **G3** versus **G4** in the presence of either **1a** or **1b**). In contrast, a reasonable kinetic resolution can be achieved if the association constants of the two isomers differ by approximately 1 order of magnitude (e.g., **G2** versus **G3** with **1a**, or **G2** versus **G4** with **1a**). The resolution is enhanced further if the binding constants for the two isomers differ by roughly 2 orders of magnitude (e.g., **G2** versus **G3** with **1b**, or **G2** versus **G4** with **1b**). The most advantageous result was observed in the kinetic resolution of **G2** and **G3** with **1b**, where approximately 97% of **G3** was still present after **G2** was fully hydrolyzed.

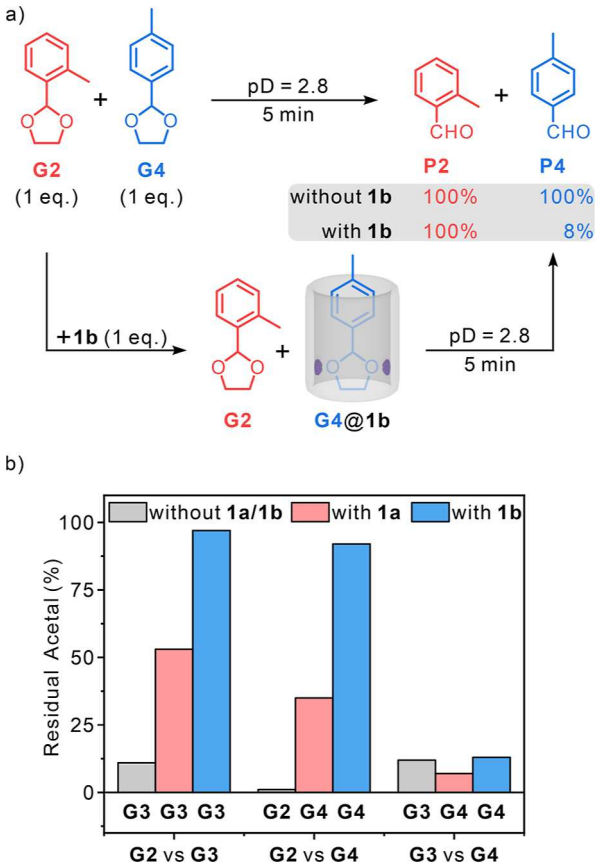

Figure 6. (a) Proposed kinetic resolution of **G2** and **G4** (0.25 mM in each) using 1.0 molar equiv of naphthotube **1b**. (b) Results of kinetic resolution studies among all the possible combinations of **G2**−**G4** by **1a** or **1b**. The bar graph shows the remaining percentage of the slower-hydrolyzing acetal as determined by NMR spectral studies under conditions where the more rapidly hydrolyzed acetal is all but completely consumed.

Additional Protection Studies. The successful non-covalent protection of acetals led us to investigate whether the present amide naphthotubes could be used to protect other reactive functionalities. The commercially available organic molecules **G11**−**G14** were chosen to test this possibility (Figure 7a). Collectively, these substrates span a range of important functional groups. For instance, the ester functional group present in **G11** is often used as a reactive intermediate and is present in a variety of perfume constituents.[73] The phosphate in **G12** is prevalent in biologically active molecules, including pesticides.[74] Dimethyl fumarate **G13** is recognized as one of the top 30 small-molecule pharmaceuticals in terms of retail sales.[75] 4-Nitrophenyl butyrate **G14** is frequently used to measure the activity of esterases.[76] All four of these substrates can be recognized by the anionic, water-soluble naphthotubes **2a** or **2b** in water (K_a as $10^3 \sim 10^6$ M^{-1}, Figures S190−S198, and Table S2). The use of these two anionic naphthotubes was expected to allow for studies of base-promoted reactions that

https://doi.org/10.1021/jacs.4c13907
J. Am. Chem. Soc. 2024, 146, 34842−34851

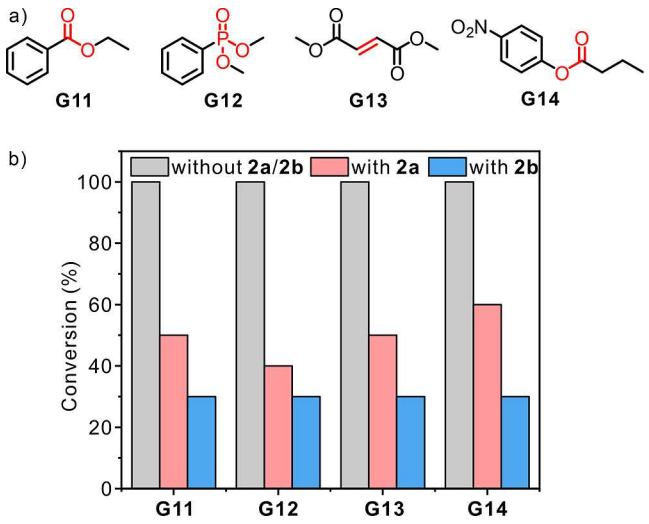

Figure 7. (a) Chemical structures of substrates **G11**–**G14**; (b) percent conversion of substrates **G11**–**G14** (0.5 mM) in the absence and presence of 1.0 molar equiv of **2a** or **2b**, determined at the point where complete conversion of the free substrate was observed. Reaction progress was monitored using ^{1}H NMR spectroscopy for substrates **G11**–**G13** and UV–vis spectroscopy in the case of **G14**. The specific reactions and conditions were as follows: For substrates **G11** and **G12**, hydrolysis was performed in deuterium oxide (D_2O) in the presence of 10 mM sodium hydroxide (NaOH) at 298 K; for **G13**, 2.0 mM mercaptoacetic acid in D_2O at pD 7.8 and 298 K was used to promote a possible addition reaction; and for **G14**, the putative hydrolysis was catalyzed by carboxylesterase EC 3.1.1.1 in water (H_2O) at pH 7.4 and 310 K.

would be difficult to monitor with the cationic systems **1a** and **1b**. Support for the proposed encapsulation, similar to that observed with guests **G1**–**G10** and naphthotubes **1a** and **1b**, was provided by DFT calculations (Figures S199–S202).

To test whether substrates **G11**–**G14** could be protected by naphthotubes **2a** and **2b**, reactions were chosen that were expected to mirror expected reactivity patterns, specifically the base-catalyzed hydrolysis of **G11** and **G12**, addition of a thiol to **G13**, and esterase-mediated hydrolysis of **G14**. Conversion was then determined by loss of initial substrate as monitored by spectroscopic means (Figures S203–S219 and Table S3). In the case of each substrate–receptor pair, conditions were chosen wherein near-complete depletion of the free substrate to the limits of detection was observed. The reactions involving **G11**–**G13** were performed in D_2O and monitored by ^{1}H NMR spectroscopy, while that of **G14** in H_2O was monitored by UV–vis spectroscopy. Under these specific reaction conditions, the presence of a naphthotube (either **2a** or **2b** at 0.5 mM) generally resulted in less than 50% substrate conversion, whereas complete conversion was observed in the absence of the host molecule (Figure 7b). Consistent with a binding-based protection mechanism analogous to that seen with **1a** and **1b** and the acetal substrates (vide supra), the level of protection for **G11**–**G14** was found to be dependent on the concentration of the host molecules **2a** and **2b** (Figure S219). Collectively, these results highlight the ability of amide naphthotubes **1a**, **1b**, **2a**, and **2b** to protect a wide range of substrates from canonical reactions otherwise expected to occur readily in aqueous media.

Given the results obtained with naphthotubes **1** and **2**, we were keen to see if other biomimetic receptors could be used to protect molecules in water. Recently, we reported a larger biomimetic receptor **4** ("amide anthryltube") that binds polar organic molecules in water effectively via a combination of hydrogen bonding and hydrophobic effects.[77] It was thus tested for its ability to promote molecular protection in water. Substrates **G15**–**G18** were selected due to their recognized utility in a variety of areas (Figure 8a). Coumarin (**G15**) serves

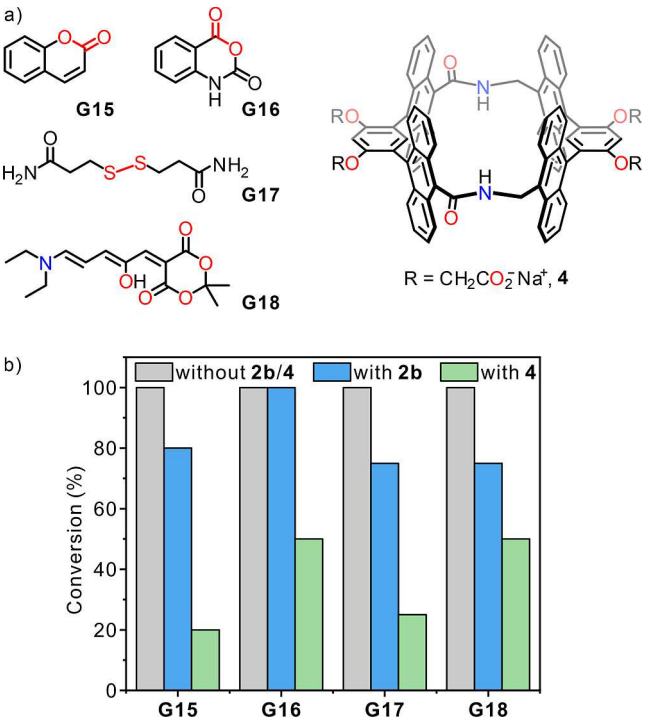

Figure 8. (a) Chemical structures of substrates **G15**–**G18**; (b) conversion of substrates **G15**–**G18** (0.5 mM) in the absence and presence of 1.0 molar equiv of **2b** or **4**, determined at the point where complete conversion of the free substrate was observed. Reaction progress was monitored using ^{1}H NMR spectroscopy. Reaction conditions: **G15** – hydrolysis with 10 mM NaOH in D_2O at 298 K; **G16** – aminolysis with 2.0 mM monoethanolamine in D_2O at pD 7.8 and 298 K; **G17** – reduction with dithiothreitol in D_2O at pD 7.8 and 298 K; **G18** – isomerization in D_2O at pD 6.9 and 298 K.

as a chromophore in a wide range of fluorescent indicators.[78] Isatoic anhydride (**G16**) is used in protein modification.[79] Disulfide bonds as embodied in substrate **G17** play a role in regulating protein structure and have seen extensive use in the area of dynamic covalent chemistry.[80,81] The donor–acceptor Stenhouse adduct **G18** is a prominent visible light-responsive photoswitch.[82]

As above, the efficacy of anthryltube **4** in protecting these substrates was tested by choosing reactions appropriate to the substrates in question, including hydrolysis of **G15**, aminolysis of **G16**, reduction of **G17**, and isomerization of **G18** (Figures 8b, S220–S235, and Table S4). It is notable that **4** exhibits superior protection to **G15**–**G18** compared with **2b**. This difference is ascribed to the presence of a larger biomimetic cavity in the case of **4**, which enables it to accommodate and protect relatively large substrates such as **G15**–**G18**. This inference is supported by the fact that higher binding affinities are seen for **G15**–**G18** in the case of the anthryltube **4** (K_a = $10^4 \sim 10^6$ M^{-1}) than the corresponding naphthotube **2b** (K_a = $10^2 \sim 10^4$ M^{-1}, Figures S236–S244 and Table S5). The optimized host–guest complex structures obtained through

https://doi.org/10.1021/jacs.4c13907
J. Am. Chem. Soc. 2024, 146, 34842–34851

DFT calculations provide support for this conclusion (Figures S245−S248). More broadly, the comparison between **4** and **2b** leads us to suggest that biomimetic receptors containing polar binding motifs, such as **1**, **2**, and **4** of the present study, can be expected to provide the best protection for those guests that they are able to accommodate most effectively. To the extent this caveat holds true, it would provide a guide to the design of new host systems targeting the protection of guests beyond the test set considered here.

CONCLUSIONS

In summary, we have shown that appropriately designed biomimetic receptors, namely the amide naphthotubes and an amide anthryltube analogue, allow for the noncovalent protection of functional organic molecules in water. The prototypical naphthotube receptors **1a** and **1b** were found to protect acetals against acid-catalyzed hydrolysis (providing half-live extensions of up to 3000-fold in the most favorable of cases). The generality of the present strategy was then validated by demonstrating its utility in protecting eight different substrates across six distinct reaction types. Here, tested substrates included ester, phosphate, disulfide, coumarin, dimethyl fumarate, isatoic anhydride, 4-nitrophenyl butyrate, and a donor−acceptor Stenhouse adduct, while the reaction types involved hydrolysis, aminolysis, addition, reduction, isomerization, and enzyme-catalyzed reactions. Of note is that receptors used in the present study can be easily recycled from the aqueous solution containing various substrates and products with high recovery rates that in the best cases exceed 80% (Figures S249−S251). We thus suggest that the encapsulation-based protection strategy outlined here could emerge as environmentally friendly and cost-effective.

ASSOCIATED CONTENT

Supporting Information

The Supporting Information is available free of charge at https://pubs.acs.org/doi/10.1021/jacs.4c13907.

Experimental details, spectroscopic information including NMR and MS, single-crystal X-ray diffraction studies, UV−vis spectroscopic studies, NMR titrations, fluorescence titrations and ITC titrations, and theoretical calculations (PDF)

Accession Codes

Deposition Numbers 2268681−2268684 contain the supplementary crystallographic data for this paper. These data can be obtained free of charge via the joint Cambridge Crystallographic Data Centre (CCDC) and Fachinformationszentrum Karlsruhe Access Structures service.

AUTHOR INFORMATION

Corresponding Authors

David Lee Phillips − *Department of Chemistry, The University of Hong Kong, Hong Kong 999077, P. R. China;* orcid.org/0000-0002-8606-8780; Email: phillips@hku.hk

Han-Yuan Gong − *College of Chemistry, Beijing Normal University, Beijing 100875, P. R. China;* orcid.org/0000-0003-4168-7657; Email: hanyuangong@bnu.edu.cn

Jonathan L. Sessler − *Department of Chemistry, The University of Texas at Austin, Austin, Texas 78712-1224, United States;* orcid.org/0000-0002-9576-1325; Email: sessler@cm.utexas.edu

Authors

Hang Zhou − *Department of Chemistry, The University of Hong Kong, Hong Kong 999077, P. R. China; Department of Chemistry, Southern University of Science and Technology, Shenzhen 518055, P. R. China;* orcid.org/0000-0002-6525-3514

Xin-Yu Pang − *Department of Chemistry, Southern University of Science and Technology, Shenzhen 518055, P. R. China;* orcid.org/0000-0002-1460-3123

Xiaojiang Xie − *Department of Chemistry, Southern University of Science and Technology, Shenzhen 518055, P. R. China;* orcid.org/0000-0003-2629-8362

Wei Jiang − *Department of Chemistry, Southern University of Science and Technology, Shenzhen 518055, P. R. China;* orcid.org/0000-0001-7683-5811

Complete contact information is available at: https://pubs.acs.org/10.1021/jacs.4c13907

Notes

The authors declare no competing financial interest.

ACKNOWLEDGMENTS

This paper is in memory of W.J. W.J. thanks Prof. Sijbren Otto at The University of Groningen for helpful discussions. We are grateful for technical support from the SUSTech Core Research Facilities and the High-Performance Computing services offered by ITS at HKU. X.X. thanks the National Natural Science Foundation of China (22274070) and the Shenzhen Municipal Science and Technology Innovation Council (20211029300007) for financial support. D.L.P. acknowledges grants from the Hong Kong Research Grants Council (GRF 17316922). H.Y.G. is grateful to the National Natural Science Foundation of China (92156009). The work in Austin was supported by the National Science Foundation (CHE-2304731) and the Robert A. Welch Foundation (F-0018).

REFERENCES

(1) Kocienski, P. J. *Protecting Groups*, 3rd ed.; Thieme: Stuttgart, 2005.

(2) Wuts, P. G. M.; Greene, T. W. *Greene's Protective Groups in Organic Synthesis*, 5th ed.; Wiley: Hoboken, 2014.

(3) Isidro-Llobet, A.; Álvarez, M.; Albericio, F. Amino Acid-Protecting Groups. *Chem. Rev.* **2009**, *109* (6), 2455−2504.

(4) Li, J.; Chen, P. R. Development and Application of Bond Cleavage Reactions in Bioorthogonal Chemistry. *Nat. Chem. Biol.* **2016**, *12* (3), 129−137.

(5) Seidi, F.; Zhong, Y.; Xiao, H.; Jin, Y.; Crespy, D. Degradable Polyprodrugs: Design and Therapeutic Efficiency. *Chem. Soc. Rev.* **2022**, *51* (15), 6652−6703.

(6) Ding, C.; Chen, C.; Zeng, X.; Chen, H.; Zhao, Y. Emerging Strategies in Stimuli-Responsive Prodrug Nanosystems for Cancer Therapy. *ACS Nano* **2022**, *16* (9), 13513−13553.

(7) Frot, T.; Volksen, W.; Purushothaman, S.; Bruce, R.; Dubois, G. Application of the Protection/Deprotection Strategy to the Science of Porous Materials. *Adv. Mater.* **2011**, *23* (25), 2828−2832.

(8) Seidi, F.; Jenjob, R.; Crespy, D. Designing Smart Polymer Conjugates for Controlled Release of Payloads. *Chem. Rev.* **2018**, *118* (7), 3965−4036.

(9) Young, I. S.; Baran, P. S. Protecting-Group-Free Synthesis as An Opportunity for Invention. *Nat. Chem.* **2009**, *1* (3), 193−205.

(10) Galan, A.; Ballester, P. Stabilization of Reactive Species by Supramolecular Encapsulation. *Chem. Soc. Rev.* **2016**, *45* (6), 1720−1737.

(11) Wang, K.; Jordan, J. H.; Hu, X. Y.; Wang, L. Supramolecular Strategies for Controlling Reactivity within Confined Nanospaces. *Angew. Chem., Int. Ed.* **2020**, *59* (33), 13712−13721.
(12) Yu, Y.; Yang, J.-M.; Rebek, J., Jr. Molecules in Confined Spaces: Reactivities and Possibilities in Cavitands. *Chem.* **2020**, *6* (6), 1265−1274.
(13) Mal, P.; Breiner, B.; Rissanen, K.; Nitschke, J. R. White Phosphorus Is Air-Stable Within a Self-Assembled Tetrahedral Capsule. *Science* **2009**, *324* (5935), 1697−1699.
(14) Jiao, T.; Chen, L.; Yang, D.; Li, X.; Wu, G.; Zeng, P.; Zhou, A.; Yin, Q.; Pan, Y.; Wu, B.; Hong, X.; Kong, X.; Lynch, V. M.; Sessler, J. L.; Li, H. Trapping White Phosphorus within a Purely Organic Molecular Container Produced by Imine Condensation. *Angew. Chem., Int. Ed.* **2017**, *56* (46), 14545−14550.
(15) Niki, K.; Tsutsui, T.; Akita, M.; Yoshizawa, M.; Yamashina, M. Recognition and Stabilization of Unsaturated Fatty Acids by a Polyaromatic Receptor. *Angew. Chem., Int. Ed.* **2020**, *59* (46), 10489−10492.
(16) Galán, A.; Gil-Ramírez, G.; Ballester, P. Kinetic Stabilization of N,N-Dimethyl-2-propyn-1-amine N-Oxide by Encapsulation. *Org. Lett.* **2013**, *15* (19), 4976−4979.
(17) Saha, R.; Devaraj, A.; Bhattacharyya, S.; Das, S.; Zangrando, E.; Mukherjee, P. S. Unusual Behavior of Donor-Acceptor Stenhouse Adducts in Confined Space of a Water-Soluble Pd^{II}_8 Molecular Vessel. *J. Am. Chem. Soc.* **2019**, *141* (21), 8638−8645.
(18) Hasegawa, S.; Meichsner, S. L.; Holstein, J. J.; Baksi, A.; Kasanmascheff, M.; Clever, G. H. Long-Lived C60 Radical Anion Stabilized Inside an Electron-Deficient Coordination Cage. *J. Am. Chem. Soc.* **2021**, *143* (26), 9718−9723.
(19) Cram, D. J.; Tanner, M. E.; Thomas, R. The Taming of Cyclobutadiene. *Angew. Chem., Int. Ed. Engl.* **1991**, *30* (8), 1024−1027.
(20) Smulders, M. M. J.; Nitschke, J. R. Supramolecular Control Over Diels-Alder Reactivity by Encapsulation and Competitive Displacement. *Chem. Sci.* **2012**, *3* (3), 785−788.
(21) Yamashina, M.; Sei, Y.; Akita, M.; Yoshizawa, M. Safe Storage of Radical Initiators within a Polyaromatic Nanocapsule. *Nat. Commun.* **2014**, *5* (1), 4662.
(22) Li, G.; Trausel, F.; van der Helm, M. P.; Klemm, B.; Breve, T. G.; van Rossum, S. A. P.; Hartono, M.; Gerlings, H.; Lovrak, M.; van Esch, J. H.; Eelkema, R. Tuneable Control of Organocatalytic Activity through Host-Guest Chemistry. *Angew. Chem., Int. Ed.* **2021**, *60* (25), 14022−14029.
(23) van der Helm, M. P.; Li, G.; Hartono, M.; Eelkema, R. Transient Host−Guest Complexation to Control Catalytic Activity. *J. Am. Chem. Soc.* **2022**, *144* (21), 9465−9471.
(24) Shi, Q.; Mower, M. P.; Blackmond, D. G.; Rebek, J., Jr. Water-Soluble Cavitands Promote Hydrolyses of Long-Chain Diesters. *Proc. Natl. Acad. Sci. U.S.A.* **2016**, *113* (33), 9199−9203.
(25) Masseroni, D.; Mosca, S.; Mower, M. P.; Blackmond, D. G.; Rebek, J., Jr. Cavitands as Reaction Vessels and Blocking Groups for Selective Reactions in Water. *Angew. Chem., Int. Ed.* **2016**, *55* (29), 8290−8293.
(26) Sun, Q.; Escobar, L.; Ballester, P. Hydrolysis of Aliphatic Bis-isonitriles in the Presence of a Polar Super Aryl-Extended Calix[4]-pyrrole Container. *Angew. Chem., Int. Ed.* **2021**, *60* (18), 10359−10365.
(27) Yebeutchou, R. M.; Dalcanale, E. Highly Selective Monomethylation of Primary Amines Through Host-Guest Product Sequestration. *J. Am. Chem. Soc.* **2009**, *131* (7), 2452−2453.
(28) Liu, S.; Gan, H.; Hermann, A. T.; Rick, S. W.; Gibb, B. C. Kinetic Resolution of Constitutional Isomers Controlled by Selective Protection Inside a Supramolecular Nanocapsule. *Nat. Chem.* **2010**, *2* (10), 847−852.
(29) Wang, K.; Jordan, J. H.; Gibb, B. C. Molecular Protection of Fatty Acid Methyl Esters within a Supramolecular Capsule. *Chem. Commun.* **2019**, *55* (78), 11695−11698.
(30) Kida, T.; Iwamoto, T.; Asahara, H.; Hinoue, T.; Akashi, M. Chiral Recognition and Kinetic Resolution of Aromatic Amines via Supramolecular Chiral Nanocapsules in Nonpolar Solvents. *J. Am. Chem. Soc.* **2013**, *135* (9), 3371−3374.
(31) Mosquera, J.; Szyszko, B.; Ho, S. K.; Nitschke, J. R. Sequence-selective Encapsulation and Protection of Long Peptides by a Self-assembled $Fe^{II}_8L_6$ Cubic Cage. *Nat. Commun.* **2017**, *8*, 14882.
(32) Chatterji, D. *Basics of Molecular Recognition*; CRC Press: Boca Raton, FL, 2016.
(33) Merlot, A. M.; Kalinowski, D. S.; Richardson, D. R. Unraveling the Mysteries of Serum Albumin—More Than Just a Serum Protein. *Front. Physiol.* **2014**, *5*, 299.
(34) Escobar, L.; Ballester, P. Molecular Recognition in Water Using Macrocyclic Synthetic Receptors. *Chem. Rev.* **2021**, *121* (4), 2445−2514.
(35) Percastegui, E. G.; Ronson, T. K.; Nitschke, J. R. Design and Applications of Water-Soluble Coordination Cages. *Chem. Rev.* **2020**, *120* (24), 13480−13544.
(36) Anslyn, E. V.; Dougherty, D. A. *Modern Physical Organic Chemistry*; University Science Books: Sausalito, CA, 2006, pp 230−232.
(37) Cremer, P. S.; Flood, A. H.; Gibb, B. C.; Mobley, D. L. Collaborative Routes to Clarifying the Murky Waters of Aqueous Supramolecular Chemistry. *Nat. Chem.* **2018**, *10* (1), 8−16.
(38) Murray, J.; Kim, K.; Ogoshi, T.; Yao, W.; Gibb, B. C. The Aqueous Supramolecular Chemistry of Cucurbit[n]urils, Pillar[n]-arenes and Deep-Cavity Cavitands. *Chem. Soc. Rev.* **2017**, *46* (9), 2479−2496.
(39) Dong, J.; Davis, A. P. Molecular Recognition Mediated by Hydrogen Bonding in Aqueous Media. *Angew. Chem., Int. Ed.* **2021**, *60* (15), 8035−8048.
(40) Escobar, L.; Sun, Q.; Ballester, P. Aryl-Extended and Super Aryl-Extended Calix[4]pyrroles: Design, Synthesis, and Applications. *Acc. Chem. Res.* **2023**, *56* (4), 500−513.
(41) Butterfield, S. M.; Rebek, J., Jr. A Synthetic Mimic of Protein Inner Space: Buried Polar Interactions in a Deep Water-Soluble Host. *J. Am. Chem. Soc.* **2006**, *128* (48), 15366−15367.
(42) Verdejo, B.; Gil-Ramirez, G.; Ballester, P. Molecular Recognition of Pyridine N-Oxides in Water Using Calix[4]pyrrole Receptors. *J. Am. Chem. Soc.* **2009**, *131* (9), 3178−3179.
(43) Escobar, L.; Diaz-Moscoso, A.; Ballester, P. Conformational Selectivity and High-Affinity Binding in the Complexation of N-phenyl Amides in Water by a Phenyl Extended Calix[4]pyrrole. *Chem. Sci.* **2018**, *9* (36), 7186−7192.
(44) Peñuelas-Haro, G.; Ballester, P. Efficient Hydrogen Bonding Recognition in Water Using Aryl-Extended Calix[4]pyrrole Receptors. *Chem. Sci.* **2019**, *10* (8), 2413−2423.
(45) Chi, X.; Zhang, H.; Vargas-Zuniga, G. I.; Peters, G. M.; Sessler, J. L. A Dual-Responsive Bola-Type Supra-amphiphile Constructed from a Water-Soluble Calix[4]pyrrole and a Tetraphenylethene-Containing Pyridine Bis-N-oxide. *J. Am. Chem. Soc.* **2016**, *138* (18), 5829−5832.
(46) Peck, E. M.; Liu, W.; Spence, G. T.; Shaw, S. K.; Davis, A. P.; Destecroix, H.; Smith, B. D. Rapid Macrocycle Threading by a Fluorescent Dye−Polymer Conjugate in Water with Nanomolar Affinity. *J. Am. Chem. Soc.* **2015**, *137* (27), 8668−8671.
(47) Liu, W.; Johnson, A.; Smith, B. D. Guest Back-Folding: A Molecular Design Strategy That Produces a Deep-Red Fluorescent Host/Guest Pair with Picomolar Affinity in Water. *J. Am. Chem. Soc.* **2018**, *140* (9), 3361−3370.
(48) Tromans, R. A.; Carter, T. S.; Chabanne, L.; Crump, M. P.; Li, H.; Matlock, J. V.; Orchard, M. G.; Davis, A. P. A Biomimetic Receptor for Glucose. *Nat. Chem.* **2019**, *11* (1), 52−56.
(49) Balduzzi, F.; Stewart, P.; Samanta, S. K.; Mooibroek, T. J.; Hoeg-Jensen, T.; Shi, K.; Smith, B. D.; Davis, A. P. A High-Affinity "Synthavidin" Receptor for Squaraine Dyes. *Angew. Chem., Int. Ed.* **2023**, *62* (48), No. e202314373.
(50) Liu, B.; Thayumanavan, S. Substituent Effects on the pH Sensitivity of Acetals and Ketals and Their Correlation with Encapsulation Stability in Polymeric Nanogels. *J. Am. Chem. Soc.* **2017**, *139* (6), 2306−2317.

(51) Wu, Y. J.; Meanwell, N. A. Geminal Diheteroatomic Motifs: Some Applications of Acetals, Ketals, and Their Sulfur and Nitrogen Homologues in Medicinal Chemistry and Drug Design. *J. Med. Chem.* **2021**, *64* (14), 9786−9874.
(52) Holloway, L. R.; Bogie, P. M.; Lyon, Y.; Ngai, C.; Miller, T. F.; Julian, R. R.; Hooley, R. J. Tandem Reactivity of a Self-Assembled Cage Catalyst with Endohedral Acid Groups. *J. Am. Chem. Soc.* **2018**, *140* (26), 8078−8081.
(53) Scorsin, L.; Roehrs, J. A.; Campedelli, R. R.; Caramori, G. F.; Ortolan, A. O.; Parreira, R. L. T.; Fiedler, H. D.; Acuna, A.; Garcia-Rio, L.; Nome, F. Cucurbituril-Mediated Catalytic Hydrolysis: A Kinetic and Computational Study with Neutral and Cationic Dioxolanes in CB7. *ACS Catal.* **2018**, *8* (12), 12067−12079.
(54) Zhang, Q.; Tiefenbacher, K. Hexameric Resorcinarene Capsule is a Brønsted Acid: Investigation and Application to Synthesis and Catalysis. *J. Am. Chem. Soc.* **2013**, *135* (43), 16213−16219.
(55) Pluth, M. D.; Bergman, R. G.; Raymond, K. N. Catalytic Deprotection of Acetals in Basic Solution with a Self-Assembled Supramolecular "Nanozyme". *Angew. Chem., Int. Ed.* **2007**, *46* (45), 8587−8589.
(56) Yang, L.-P.; Wang, X.; Yao, H.; Jiang, W. Naphthotubes: Macrocyclic Hosts with a Biomimetic Cavity Feature. *Acc. Chem. Res.* **2020**, *53* (1), 198−208.
(57) Ke, H.; Yang, L.-P.; Xie, M.; Chen, Z.; Yao, H.; Jiang, W. Shear-Induced Assembly of a Transient Yet Highly Stretchable Hydrogel based on Pseudopolyrotaxanes. *Nat. Chem.* **2019**, *11* (5), 470−477.
(58) Huang, G.-B.; Wang, S.-H.; Ke, H.; Yang, L.-P.; Jiang, W. Selective Recognition of Highly Hydrophilic Molecules in Water by Endo-Functionalized Molecular Tubes. *J. Am. Chem. Soc.* **2016**, *138* (44), 14550−14553.
(59) Yao, H.; Ke, H.; Zhang, X.; Pan, S.-J.; Li, M.-S.; Yang, L.-P.; Schreckenbach, G.; Jiang, W. Molecular Recognition of Hydrophilic Molecules in Water by Combining the Hydrophobic Effect with Hydrogen Bonding. *J. Am. Chem. Soc.* **2018**, *140* (41), 13466−13477.
(60) Yang, L. P.; Ke, H.; Yao, H.; Jiang, W. Effective and Rapid Removal of Polar Organic Micropollutants from Water by Amide Naphthotube-Crosslinked Polymers. *Angew. Chem., Int. Ed.* **2021**, *60* (39), 21404−21411.
(61) Wang, L.-L.; Quan, M.; Yang, T.-L.; Chen, Z.; Jiang, W. A Green and Wide-Scope Approach for Chiroptical Sensing of Organic Molecules through Biomimetic Recognition in Water. *Angew. Chem., Int. Ed.* **2020**, *59* (52), 23817−23824.
(62) Sarkar, S.; Ballester, P.; Spektor, M.; Kataev, E. A. Micromolar Affinity and Higher: Synthetic Host-Guest Complexes with High Stabilities. *Angew. Chem., Int. Ed.* **2023**, *62* (28), No. e202214705.
(63) Rekharsky, M. V.; Inoue, Y. Complexation Thermodynamics of Cyclodextrins. *Chem. Rev.* **1998**, *98* (5), 1875−1917.
(64) Crini, G. Review: A History of Cyclodextrins. *Chem. Rev.* **2014**, *114* (21), 10940−10975.
(65) Barrow, S. J.; Kasera, S.; Rowland, M. J.; del Barrio, J.; Scherman, O. A. Cucurbituril-Based Molecular Recognition. *Chem. Rev.* **2015**, *115* (22), 12320−12406.
(66) Kim, K.; Selvapalam, N.; Ko, Y. H.; Park, K. M.; Kim, D.; Kim, J. Functionalized Cucurbiturils and Their Applications. *Chem. Soc. Rev.* **2007**, *36* (2), 267−279.
(67) Kloeck, C.; Dsouza, R. N.; Nau, W. M. Cucurbituril-Mediated Supramolecular Acid Catalysis. *Org. Lett.* **2009**, *11* (12), 2595−2598.
(68) Scheiner, S.; Čuma, M. Relative Stability of Hydrogen and Deuterium Bonds. *J. Am. Chem. Soc.* **1996**, *118* (6), 1511−1521.
(69) Čuma, M.; Scheiner, S. Influence of Isotopic Substitution on Strength of Hydrogen Bonds of Common Organic Groups. *J. Phys. Org. Chem.* **1997**, *10* (5), 383−395.
(70) Scheiner, S. *Hydrogen Bonding. A Theoretical Perspective*; Oxford University Press: Oxford, U.K., 1997.
(71) Rekharsky, M. V.; Inoue, Y. Solvent and Guest Isotope Effects on Complexation Thermodynamics of α-, β-, and 6-Amino-6-deoxy-β-cyclodextrins. *J. Am. Chem. Soc.* **2002**, *124* (41), 12361−12371.
(72) Biedermann, F.; Vendruscolo, M.; Scherman, O. A.; De Simone, A.; Nau, W. M. Cucurbit[8]uril and Blue-Box: High-Energy Water Release Overwhelms Electrostatic Interactions. *J. Am. Chem. Soc.* **2013**, *135* (39), 14879−14888.
(73) SÁ, A. G. A.; de Meneses, A. C.; de Araújo, P. H. H.; de Oliveira, D. A Review on Enzymatic Synthesis of Aromatic Esters Used as Flavor Ingredients for Food, Cosmetics and Pharmaceuticals Industries. *Trends Food Sci. Technol.* **2017**, *69*, 95−105.
(74) Kim, K.; Tsay, O. G.; Atwood, D. A.; Churchill, D. G. Destruction and Detection of Chemical Warfare Agents. *Chem. Rev.* **2011**, *111* (9), 5345−5403.
(75) McGrath, N. A.; Brichacek, M.; Njardarson, J. T. A Graphical Journey of Innovative Organic Architectures That Have Improved Our Lives. *J. Chem. Educ.* **2010**, *87* (12), 1348−1349.
(76) Pliego, J.; Mateos, J. C.; Rodriguez, J.; Valero, F.; Baeza, M.; Femat, R.; Camacho, R.; Sandoval, G.; Herrera-Lopez, E. J. Monitoring Lipase/Esterase Activity by Stopped Flow in A Sequential Injection Analysis System Using *p*-Nitrophenyl Butyrate. *Sensors* **2015**, *15* (2), 2798−2811.
(77) Zhou, H.; Pang, X. Y.; Wang, X.; Yao, H.; Yang, L. P.; Jiang, W. Biomimetic Recognition of Quinones in Water by an Endo-Functionalized Cavity with Anthracene Sidewalls. *Angew. Chem., Int. Ed.* **2021**, *60* (49), 25981−25987.
(78) Cao, D.; Liu, Z.; Verwilst, P.; Koo, S.; Jangjili, P.; Kim, J. S.; Lin, W. Coumarin-Based Small-Molecule Fluorescent Chemosensors. *Chem. Rev.* **2019**, *119* (18), 10403−10519.
(79) Hooker, J. M.; Esser-Kahn, A. P.; Francis, M. B. Modification of Aniline Containing Proteins Using an Oxidative Coupling Strategy. *J. Am. Chem. Soc.* **2006**, *128* (49), 15558−15559.
(80) Fass, D.; Thorpe, C. Chemistry and Enzymology of Disulfide Cross-Linking in Proteins. *Chem. Rev.* **2018**, *118* (3), 1169−1198.
(81) Black, S. P.; Sanders, J. K. M.; Stefankiewicz, A. R. Disulfide Exchange: Exposing Supramolecular Reactivity Through Dynamic Covalent Chemistry. *Chem. Soc. Rev.* **2014**, *43* (6), 1861−1872.
(82) Helmy, S.; Leibfarth, F. A.; Oh, S.; Poelma, J. E.; Hawker, C. J.; Read de Alaniz, J. Photoswitching Using Visible Light: A New Class of Organic Photochromic Molecules. *J. Am. Chem. Soc.* **2014**, *136* (23), 8169−8172.

https://doi.org/10.1021/jacs.4c13907
J. Am. Chem. Soc. 2024, 146, 34842−34851